

# **Title: Advances in the Molecular Understanding of GPCR-Arrestin Complexes**

**Authors:** Ivana Petrovic<sup>1</sup>, Stephan Grzesiek<sup>1, \*</sup>, Polina Isaikina<sup>2, \*</sup>

## **Affiliations:**

1 Biozentrum, University of Basel, CH-4056 Basel, Switzerland

2 Center for Life Sciences, Paul Scherrer Institut, CH-5232 Villigen, Switzerland

Keywords: arrestin; G protein-coupled receptor (GPCR); phosphorylation; signaling; internalization;

\*Address correspondence to:

Polina Isaikina  
polina.isaikina@psi.ch  
Center for Life Sciences  
Paul Scherrer Institut  
CH-5232 Villigen, Switzerland

Stephan Grzesiek  
stephan.grzesiek@unibas.ch  
Biozentrum  
University of Basel  
CH-4056 Basel, Switzerland

## **Abstract**

Arrestins are essential proteins for the regulation of G protein-coupled receptors (GPCRs). They mediate GPCR desensitization after the activated receptor has been phosphorylated by G protein receptor kinases (GRKs). In addition, GPCR-arrestin interactions may trigger signaling pathways that are distinct and independent from G proteins. The non-visual GPCRs encompass hundreds of receptors with varying phosphorylation patterns and amino acid sequences, which are regulated by only two human non-visual arrestin isoforms. This review describes recent findings on GPCR-arrestin complexes, obtained by structural techniques, biophysical, biochemical, and cellular assays. The solved structures of complete GPCR-arrestin complexes are of limited resolution ranging from 3.2 to 4.7 Å and reveal a high variability in the relative receptor-arrestin orientation. In contrast, biophysical and functional data indicate that arrestin recruitment, activation and GPCR-arrestin complex stability depend on the receptor phosphosite sequence patterns and density. At present, there is still a manifest lack of high-resolution structural and dynamical information on the interactions of native GPCRs with both GRKs and arrestins, which could provide a detailed molecular understanding of the genesis of receptor phosphorylation patterns and the specificity GPCR-arrestin interactions. Such insights seem crucial for progress in the rational design of advanced, arrestin-specific therapeutics.

## Introduction

Arrestins are a small family of cytosolic proteins that play a crucial role in the regulation of G protein-coupled receptors (GPCRs) by controlling receptor desensitization (1) and mediating subsequent signaling events (2). Arrestins interact with GPCRs upon phosphorylation of their C-terminal tail or intracellular loops by GPCR kinases (GRKs) (3). This interaction promotes the sequestration of the receptor from the plasma membrane and facilitates its internalization. Once bound to the receptor, arrestins can also initiate independent signaling pathways (4), thereby regulating various cellular processes such as cell proliferation (5) and transcription (6).

In humans, four genetically and structurally conserved arrestin subtypes regulate hundreds of GPCRs with poorly conserved sequences and varying phosphorylation patterns. These subtypes include the visual arrestins (arrestin1 and arrestin4), which are expressed in the retina rods and cones and regulate only photoreceptors, and the non-visual arrestins (arrestin2 and arrestin3, formerly known as  $\beta$ -arrestin1 and  $\beta$ -arrestin2) (7), which are expressed in all other tissues and cell types, interacting with hundreds of different GPCRs. This raises the fundamental question: How can only two arrestin isoforms recognize and bind so many different GPCRs?

A barcode hypothesis has been put forward in an attempt to explain how different phosphorylation patterns recognized by the two non-visual arrestins lead to distinct functional outcomes (8–10). The hypothesis posits that the presence or absence of specific phosphorylation sites arranged in a particular manner induces differences in the receptor-arrestin interaction and the subsequent cellular response. In support of this hypothesis, arrestin binding and conformational changes have been shown to depend more on the arrangement of phosphates than their total number (11). Recent studies have revealed the existence of specific phosphorylation motifs embedded within the receptor C-terminal tail or intracellular loops that recruit arrestins to a certain receptor (12–16). However, the complexity and dynamic character of the GPCR interactions with arrestins and GRKs have so far prevented the observation of the signaling interactions at atomic resolution.

Knowledge on the receptor-arrestin interactions has been obtained primarily by functional assays and structural studies. Functional assays typically monitor arrestin recruitment to GPCRs as a function of ligand (17) or GRK subtype (18) within cells. Structural studies using mainly cryo-EM (19–26), X-ray crystallography (12,27), molecular dynamics (MD) simulations (11,28,29), FRET (30), or NMR (31) aim to resolve changes in the arrestin and receptor conformations during complex formation. Due to the transient nature of receptor-arrestin interactions and their intrinsic structural mobility, obtaining high-resolution structural information on the full-length complexes is challenging. Thus, structural studies have often been restricted to arrestin complexes with phosphopeptides mimicking the native C-terminal tail of a given GPCR.

Generally, crystallographic structures of phosphopeptide-arrestin complexes have higher resolution than structures obtained by single-particle cryo-EM. They have delineated the individual phosphosites involved in the interaction from various receptors such as V2R (32), CCR5 (13) or ACKR3 (14). Moreover, due to their smaller size, the phosphopeptide-arrestin complexes are also easier to study by NMR, which has provided unique atom-scale dynamic and structural information about their interactions (13,15,33) in the absence of stabilizing antibody fragments. The latter are often used in crystallographic or cryo-EM studies but may potentially bias the system.

In this review, we describe the currently available structural and functional data on phosphorylation-governed GPCR-arrestin interactions. The overview demonstrates that an integrative approach is necessary to further expand our understanding of these important molecular complexes.

### **Receptor phosphorylation preceding arrestin binding**

The seven mammalian GRKs phosphorylate and regulate hundreds of GPCRs. These can be further separated into three subfamilies: GRK1 (GRK1 and GRK7), GRK2 (GRK2 and GRK3), and GRK4 (GRK4, GRK5 and GRK6). The basic structure is conserved across all GRKs and

comprises a short N-terminal  $\alpha$ -helical domain ( $\alpha$ N-helix), a regulatory domain, and a catalytic (kinase) domain with an ATP binding site embedded between the N-terminal small lobe and C-terminal large lobe. The very C-terminus of GRKs mediates membrane localization via prenylation (GRK1 and GRK7), palmitoylation (GRK4 and GRK6), or direct lipid binding either via a pleckstrin homology domain (GRK2 and GRK3) or a polybasic/hydrophobic domain (GRK5) (3).

The interaction of GRKs with many different receptors is enabled by their low sequence/structural specificity (3) and their ability to phosphorylate various peptides in the absence of the receptor transmembrane domain (34). Despite their crucial role, only two structures of GPCR-GRK complexes (35,36) have been solved by cryo-EM. Neither of them contains resolved density for the receptor C-terminal tail. Thus, high-resolution information about site-specific interactions between the kinase and potential phosphosites is currently missing and site-specific information on GPCR phosphorylation by GRKs has mainly been obtained by mass spectrometry or phosphospecific antibodies.

Heterogeneities in the degree of serine and threonine phosphorylation have been observed for the neurotensin receptor 1 (NTR1) phosphorylated by GRK5 (20) and for the CC chemokine receptor 5 (CCR5) phosphorylated by GRK2 (13), respectively. Such variations in the phosphorylation patterns have been shown to activate distinct arrestin-mediated ERK1/2 signaling pathways (37).

Recent studies have also addressed the overall impact of individual GRKs on arrestin recruitment and GPCR regulation (18,38) in GRK-knockout cell lines generated by the CRISPR/Cas9 technology (39). Using this strategy, it was shown that GRK6 induces the highest recruitment of arrestin3 to the  $\beta$ 2-adrenergic receptor ( $\beta$ 2AR) (18) and that GRK2 is more important than GRK3 for arrestin3 recruitment to the  $\mu$ -opioid receptor ( $\mu$ OR) (38). However, these studies also reveal that depending on the specific GPCR, different GRK isoforms may lead to similar arrestin interactions. This introduces another layer of complexity to the modulation of

GPCR signaling and trafficking. Therefore, more specifically designed experiments are needed to provide a comprehensive picture of specific GPCR phosphorylation, its relation to arrestin binding modes, and the subsequent cellular consequences.

### **Structures of GPCR-arrestin complexes**

In stark contrast to the more than 500 solved GPCR-G protein complex structures, only a limited number of GPCR complex structures with GRKs or arrestins are currently available (40) (Figure 1A).

Initial structural studies suggested two modes of arrestin coupling to a phosphorylated GPCR: a tail-engaged complex, where arrestin binds solely to a receptor's phosphorylated tail, and a core-engaged complex, likely formed by the further insertion of arrestin into the transmembrane core of a GPCR (31,41,42).

The first structure of active arrestin2 was obtained by forming a complex with the C-terminal V2R phosphopeptide and a stabilizing Fab fragment (Fab30). It was solved in 2013 by X-ray crystallography and provided crucial insights into the molecular basis of arrestin2 activation by this receptor C-terminal phosphopeptide (32). Specifically, arrestin activation involves the formation of the anti-parallel  $\beta$ -sheet between the arrestin strand  $\beta$ 1 and the receptor phosphopeptide, which replaces strand  $\beta$ 20 in the parallel  $\beta$ -sheet of the apo arrestin2, disrupting the polar core formed by a network of highly conserved ionic interactions (Figure 1B). This triggers conformational changes in key arrestin core loops, such as the lariat, finger, and middle loops, and induces a twist of about  $20^\circ$  in the C-domain relative to the N-domain. These rearrangements are crucial for arrestin activation and its subsequent receptor interaction. The activated arrestin then inserts into the receptor's transmembrane bundle via its finger loop. While the hallmarks of arrestin activation are generally conserved across arrestin isoforms, the degree of interdomain twist and conformation of the central crest loops can vary depending on the specific phosphopeptide, lipid composition and arrestin subtype involved (13,14,16,33,43).

In 2015, the first full-length receptor structure of human rhodopsin bound to mouse rod arrestin was solved using XFEL technology. Initially, this structure offered limited resolution and the phosphorylation sites on the C-terminal tail were not resolved. Subsequent refinements, however, improved the overall resolution and enabled the modeling of phosphorylated residues within the electron density, which suggested a certain phosphorylation barcode [pX(X)pXXp] responsible for arrestin recruitment (Figure 2A) (12).

For several years, no further high-resolution structures of GPCR-arrestin complexes were solved until additional cryo-EM hardware and software improvements made it possible to obtain higher-resolution structures of more dynamic and transient GPCR complexes and obviated the need for sample crystallization (44).

Until present, this technical progress has provided an additional eight structures of unique receptor-arrestin2 complexes (Figure 2B,C) (19–26). Due to the weakness of the arrestin interactions with native receptors, most of the receptor-arrestin complexes have been solved as receptor fusions with the non-native C-terminal tail of V2R, which is known for its high affinity and efficient activation of arrestin2. However, this commonly used strategy prevents a direct assessment of the structural impact of native receptor phosphorylation on the arrestin interactions. In addition, the complexes are often stabilized by Fab30 (19,23,24) or its derivatives (21,22,25,26), which may potentially bias the arrestin conformations.

Notably, the arrestin2 structures in complex with V2R (22) and NT1R (20) are the only arrestin2-receptor high-resolution structures containing native receptor C-terminal tails. The V2R-arrestin2 complex had been stabilized by the single-chain Fab30 derivative (scFv30) and the NT1R-arrestin2 complex chemically cross-linked, respectively. Whereas the phosphosites were modeled in the V2R-arrestin2 complex, this was not the case for the NT1R-arrestin2 complex. Remarkably, the latter structure shows a clear density for a phosphatidylinositol 4,5-bisphosphate (PIP2) derivative, mediating the receptor interaction with the arrestin2 C-domain (20,45).

Other arrestin complexes with native wild-type receptors featuring different phosphorylation motifs or extended loops present a challenge for high-resolution structural analysis. The inherent difficulties in capturing these interactions are exemplified by the low-resolution cryo-EM density of the native muscarinic receptor 2 (M2R) complexed with arrestin2 (Figure 2B) (24). Structures of arrestin complexes with phosphorylated GPCR C-terminal tail peptides solved by X-ray crystallography have provided higher resolution, thereby revealing the exact position and coordination of several phosphosites important for arrestin interaction (13,14,32).

In addition to complex structures with arrestin fully engaged with the receptor core, also structures with arrestin bound only to the receptor tail have been reported (Figure 2C) (26,46). These include the active  $\beta$ 2-adrenergic receptor ( $\beta$ 2AR) with its C-terminal tail replaced by the V2R tail, which was found to simultaneously bind the heterotrimeric Gs heterotrimer via core and arrestin2 via tail interactions (46). This complex had additionally been stabilized by two nanobodies and Fab30. Another important set of arrestin2 complex structures involves the V2R tail-fused class B GPCR glucagon receptor (GCGR) in the apo state or bound to the glucagon agonist. In both cases, arrestin2 coupled to the V2R tail, but not to the receptor core (26). Surprisingly, the GCGR remained in the inactive conformation in both complexes, indicating that the arrestin2 engagement only required phosphorylation of the receptor tail, but not an opening of the receptor intracellular cavity. These  $\beta$ 2AR and GCGR complex structures provide examples of high-resolution tail-engaged complexes, which have also been observed in other GPCR-arrestin EM studies (47) but were conformationally too heterogeneous for high-resolution reconstruction (48).

To date, no high-resolution structure of a receptor coupled to arrestin3 has been deposited in the Protein Data Bank (PDB), indirectly confirming the transient nature of arrestin3 interactions. Recently, however, the cryo-EM structure of the atypical chemokine receptor 3 (ACKR3) in complex with arrestin3 binding only to the C-terminal receptor tail has been reported as a preprint (49). Despite using a novel Fab fragment for stabilization, the resolution



of this complex remains limited, allowing only the high-resolution structural refinement of the arrestin3-Fab part of the complex.

### **The multiple faces of arrestin coupling**

Despite the similar stabilization strategies, which may introduce biases, the described arrestin2 complexes exhibit a significant variability in the arrestin2-receptor orientations (Figure 2D). These comprise up to 90° rotations around the vertical axis (taken in the direction of the membrane normal) and tilts along this axis by up to 25°. This indicates a poor conservation of arrestin interactions with the receptor core and contrasts the G protein-bound structures where almost always an identical engagement of the receptor with the G protein is observed (50).

This variability in arrestin's relative orientation strongly correlates with conformational changes of the loops in the central crest region. These loops directly interact with the receptor, and the interaction interface differs significantly depending on its orientation. Notably, the finger loop, which directly inserts into a transmembrane bundle of the receptor, can adopt a helical structure or random coil conformation, influencing the depth of insertion of arrestin to some degree (Figure 2D). In the tail-engaged complexes of the glucagon receptor, this loop does not insert into the transmembrane bundle. Instead, it interacts with helix VIII of the receptor, located near the C-terminal tail (Figure 2C, right). This illustrates the overall structural plasticity of arrestin.

Recent studies have further elucidated the role of phosphoinositides like PIP<sub>2</sub>, in GPCR-arrestin complexes (20,45,22,26,51). It was demonstrated that arrestin2 can spontaneously pre-associate with the plasma membrane, primarily through its C-edge (51), where it engages with PIP<sub>2</sub>, forming multiple ionic interactions with basic residues in the C-lobe, a known inositol phosphate binding site (20,22,26). This pre-association is crucial as it facilitates the lateral diffusion of arrestin's on the membrane, allowing it to interact with receptors more efficiently. While stabilizing, these interactions do not seem to dictate the overall mode of arrestin

engagement with the receptor. For example, while the PIP2 derivative is present in the NT1R-arrestin complex (20), where arrestin2 fully engages with the receptor core, similar interactions with the PIP2 derivative are observed in the GCGR-arrestin complex, where arrestin primarily engages with the receptor tail (26). This suggests that lipid interactions like those with PIP2 are crucial for stabilizing the complex, but they do not solely determine the specific engagement mode of arrestin with different receptors.

The specific orientation of arrestin relative to the receptor seems to result from particular but relatively weak interactions. Thus independently solved structures of the same receptors coupled to arrestin2, such as NT1R (20,52) and cannabinoid receptor 1 (CB1R) (23,53), exhibit variations of about 15° (Figure 2E), which may be the result of variations in the complex stabilization strategies or receptor phosphorylation procedures. Conversely, the M2R-arrestin2 and CB1R-arrestin2 complexes embedded in lipid nanodiscs and detergent, respectively, adopt a similar orientation (Figure 2B,D), which may indicate that the variability of the arrestin complexes is not strongly influenced by the lipid environment.

### **The role of conserved motifs in arrestin binding**

In support of the barcode hypothesis (8–10), several arrestin isoform-specific recognition phosphorylation patterns have been suggested. Initially, the pX(X)pXXp barcode had been proposed for arrestin1 (12), which was later adjusted to pXXp (15). Then, a pXXpXXp motif has been proposed for arrestin3 (14). More recently, pXpp has been proposed as a key motif for arrestin2 binding and activation (13,16), which may also be important for the arrestin3 interaction (16).

To document the prevalence of the pXpp motif, we analyzed the sequences of the C-terminal tail and intracellular loop 3 (ICL3) of all human GPCRs whose sequences are available in the GPCRdb (<https://gpcrdb.org/>). Out of over 400 GPCR sequences examined (Figure 3, Table S1), nearly half of the receptors feature at least one pXpp motif. This motif predominantly occurs in the receptor C-terminal tail. However, for some receptor classes (5-hydroxytryptamine

receptors, muscarinic receptors,  $\alpha$ -adrenergic receptors, and histamine receptors), the motif is almost exclusively found in ICL3. Remarkably, the interacting ICL3 phosphosites constitute a pXpp motif in a recent low-resolution structure of native M2R in complex with arrestin2 (24). Of note, very few receptors contain pXpp in both ICL3 and the C-terminal tail, suggesting that their contribution towards arrestin interaction is mutually exclusive.

The functional significance of individual phosphorylation sites within the pXpp motif has been demonstrated by solution NMR spectroscopy for arrestin2-CCR5 phosphopeptide complexes (13). In this study, the contributions of individual phosphoresidues to arrestin binding and activation were quantified, and their significance was further confirmed by cellular assays. A further analysis of V2R phosphopeptides using fluorescence anisotropy, NMR, and biochemical assays has revealed distinct classes of phosphorylation sites responsible for arrestin1-3 interactions (15). The pattern responsible for arrestin2 interaction is compatible with the pXpp motif.

Interestingly, many receptors bearing the pXpp motif in their C-terminal tail are peptide-binding GPCRs. Given that the presence of the pXpp motif strongly correlates with robust arrestin recruitment (13), we hypothesize that the pXpp motif may drive efficient clearance of peptide ligands from the cell surface.

## **Summary and future directions**

GPCRs activate diverse signaling pathways by coupling to various intracellular partners such as G proteins, GRKs, and arrestins. Arrestin interactions are more transient than those of G proteins and are modulated by intracellular phosphorylation via GRKs. While commonly used strategies for solving structures of GPCR-arrestin complexes by receptor fusion to strong phosphopeptide binders have provided valuable insights, they have precluded the direct assessment of the influence of native receptor phosphorylation on arrestin binding and conformation.

A deeper understanding of arrestin signaling will require (i) clarifying the determinants of GRK isoform recognition and receptor phosphorylation levels, (ii) obtaining additional structures of native receptors coupled to arrestin2 or arrestin3 to derive general principles of receptor arrestin interactions from a solid statistical basis, (iii) analysis by NMR, time-resolved cryo-EM or X-ray crystallography, or other methods for a comprehensive description of the dynamics of the GPCR-kinase and -arrestin interactions, (iv) elucidating the role of the membrane, including its chemical composition and physical properties, in GPCR-GRK and -arrestin interactions (51). Such a broad, high-resolution molecular understanding of arrestin signaling may be crucial for progress in the rational design of advanced, arrestin-specific therapeutics.

## **Perspectives**

- GPCRs are the largest and most diverse group of membrane receptors. Arrestins regulate GPCRs by controlling receptor desensitization and mediating subsequent signaling events.
- While commonly used strategies for solving structures of GPCR-arrestin complexes by receptor fusion to strong phosphopeptide binders have provided valuable insights, they have precluded the direct assessment of the influence of native receptor phosphorylation on arrestin binding and conformation.
- Further elucidation of the dynamics of GPCR-kinase and -arrestin interactions using NMR, time-resolved cryo-EM, X-ray crystallography, or other advanced methods are needed to describe native GPCR regulation by GRKs and arrestins comprehensively. Such a broad, high-resolution molecular understanding of arrestin signaling may be crucial for progress in the rational design of advanced, arrestin-specific therapeutics.

## **Competing interest**

The authors declare that there are no competing interests associated with the manuscript.

## **Funding**

This work is supported by the Swiss National Science Foundation grants 31-201270 and IZLIZ3-200298 to S.G., a Paul Scherrer Institute Research Grant to P.I., and a Fellowship for Excellence by the Biozentrum Basel International PhD Program to I.P.

## **Abbreviations**

5HT2bR – 5-Hydroxytryptamine (serotonin) receptor 2B

ACKR – Atypical chemokine receptor

$\beta$ AR – Beta-adrenergic receptor

CB1R – Cannabinoid receptor 1

CCR5 – CC chemokine receptor 5

Cryo-EM – Cryogenic electron microscopy

EMDB – Electron Microscopy Data Bank

FRET – Förster resonance energy transfer

GPCR – G protein-coupled receptor

GRK – G protein-coupled receptor kinase

ICL – Intracellular loop

M2R – Muscarinic acetylcholine receptor 2

NMR – Nuclear Magnetic Resonance

NT1R – Neurotensin receptor 1

PDB – Protein Data Bank

V2R – Vasopressin receptor 2

V2Rpp – Vasopressin receptor 2 C-terminal phosphopeptide

XFEL – X-ray free-electron laser

## Figures

**Figure 1. Structural features of arrestin activation and diversity of the GPCR signaling partners (A)** Diversity of the GPCR signaling partners and number of available complex structures (as of June 2024) for each signaling subtype. The Figure illustrates the vast array of G proteins, featuring 16  $\alpha$  subunits, 5  $\beta$  subunits, and 11  $\gamma$  subunits (54), offering numerous binding combinations and increased specificity. This often results in more stable complexes, especially under nucleotide-free conditions. In contrast, the diversity narrows significantly for subsequent binding partners with only 7 GRKs (two specialized for the visual system) and 4 arrestins (two visual). The concomitant decreased specificity is expected to reduce the complex stability, which is reflected in the fewer solved structures. **(B)** Structural transitions during arrestin activation. The left panel illustrates the apo (inactive) form of human arrestin2 (PDB:8AS4), highlighting key structural elements including the finger loop, middle loop, lariat loop, and strands  $\beta$ 1 and  $\beta$ 20 in the C-domain. Upon binding to the C-terminal GPCR phosphopeptide (PDB:8AS3), the strand  $\beta$ 20 is replaced by the phosphopeptide, leading to significant conformational changes in the central loops (lariat, finger, and middle loops) and a twist in the C-domain relative to the N-domain.

**Figure 2. X-ray and cryo-EM structures of unique GPCR-arrestin complexes and their analysis. (A)** Electron density of rhodopsin-arrestin1 complex solved by XFEL (PDB: 5W0P). **(B-E)** Cryo-EM densities and detailed models of various GPCR-arrestin2 complexes. **(B)** Core engaged-complexes: V2R (EMDB-14221; PDB:7R0C), NT1R (EMDB-20836; PDB:6UP7), M2R-V2Rpp (EMDB-20612; PDB:6U1N), M2R native (EMDB-36093), CB1R-V2Rpp (EMDB-37849; PDB:8WU1),  $\beta$ 1AR-V2Rpp (EMDB-10515; PDB:6TKO), 5HT2bR-modified (EMDB-25403; PDB:7SRS). **(C)** Tail-engaged complexes:  $\beta$ 2AR-V2Rpp megaplex (EMDB-9375 and 9376; PDB:6NI2 and 6NI3); apo GCGR-V2Rpp (EMDB-36606; PDB:8JRU), glucagon-bound GCRG-V2Rpp (EMDB-36607; PDB:8JRV). In both GCGR structures, this class B receptor remains in an inactive conformation and is coupled to arrestin only via the C-terminal tail. Structural resolutions are indicated in panels (A-C). **(D)** Structural alignment of arrestin2-core-engaged complexes. The arrestin2 color corresponds to the associated receptor chain from panel B. The complexes were aligned on the receptor chain and only one chain is displayed (grey) for simplicity. **(E)** Structural comparison of identical receptor complexes with arrestin2: NT1R (PDB:6UP7 and 6PWC) and CB1R-V2Rpp (PDB:8WU1 and 8WRZ).

**Figure 3. The pXpp motif across various receptor classes.** Presence of the pXpp motif in ICL3 or C-terminal receptor tail (C-term) as derived from the GPCR sequences available in the GPCRdb. The receptors follow the GPCRdb classification. The occurrence of at least one pXpp motif is marked with an 'x'.

## References

1. Rajagopal S, Shenoy SK. GPCR desensitization: Acute and prolonged phases. *Cellular Signalling*. 2018 Jan 1;41:9–16. <https://doi.org/10.1016/j.cellsig.2017.01.024>
2. Gurevich VV, Gurevich EV. GPCR Signaling Regulation: The Role of GRKs and Arrestins. *Frontiers in Pharmacology* [Internet]. 2019 [cited 2023 Aug 31];10.
3. Komolov KE, Benovic JL. G protein-coupled receptor kinases: Past, present and future. *Cellular Signalling*. 2018 Jan 1;41:17–24. <https://doi.org/10.1016/j.cellsig.2017.07.004>
4. Jean-Charles PY, Kaur S, Shenoy SK. GPCR signaling via  $\beta$ -arrestin-dependent mechanisms. *J Cardiovasc Pharmacol*. 2017 Sep;70(3):142–58. <https://doi.org/10.1097/FJC.0000000000000482>
5. Yu H, Wang M, Zhang T, Cao L, Li Z, Du Y, et al. Dual roles of  $\beta$ -arrestin 1 in mediating cell metabolism and proliferation in gastric cancer. *Proc Natl Acad Sci U S A*. 2022 Oct 4;119(40):e2123231119. <https://doi.org/10.1073/pnas.2123231119>
6. Barella LF, Rossi M, Pydi SP, Meister J, Jain S, Cui Y, et al.  $\beta$ -Arrestin-1 is required for adaptive  $\beta$ -cell mass expansion during obesity. *Nat Commun*. 2021 Jun 7;12(1):3385. <https://doi.org/10.1038/s41467-021-23656-1>
7. Gurevich EV, Gurevich VV. Arrestins: ubiquitous regulators of cellular signaling pathways. *Genome Biology*. 2006 Oct 2;7(9):236. <https://doi.org/10.1186/gb-2006-7-9-236>
8. Nobles KN, Xiao K, Ahn S, Shukla AK, Lam CM, Rajagopal S, et al. Distinct phosphorylation sites on the  $\beta$ (2)-adrenergic receptor establish a barcode that encodes differential functions of  $\beta$ -arrestin. *Sci Signal*. 2011 Aug 9;4(185):ra51. <https://doi.org/10.1126/scisignal.2001707>
9. Butcher AJ, Prihandoko R, Kong KC, McWilliams P, Edwards JM, Bottrill A, et al. Differential G-protein-coupled Receptor Phosphorylation Provides Evidence for a Signaling Bar Code\*. *Journal of Biological Chemistry*. 2011 Apr 1;286(13):11506–18. <https://doi.org/10.1074/jbc.M110.154526>
10. Kim J, Ahn S, Ren XR, Whalen EJ, Reiter E, Wei H, et al. Functional antagonism of different G protein-coupled receptor kinases for  $\beta$ -arrestin-mediated angiotensin II receptor signaling. *Proceedings of the National Academy of Sciences*. 2005 Feb;102(5):1442–7. <https://doi.org/10.1073/pnas.0409532102>
11. Latorraca NR, Masureel M, Hollingsworth SA, Heydenreich FM, Suomivuori CM, Brinton C, et al. How GPCR Phosphorylation Patterns Orchestrate Arrestin-Mediated Signaling. *Cell*. 2020 Dec;183(7):1813–1825.e18. <https://doi.org/10.1016/j.cell.2020.11.014>
12. Zhou XE, He Y, de Waal PW, Gao X, Kang Y, Van Eps N, et al. Identification of Phosphorylation Codes for Arrestin Recruitment by G Protein-Coupled Receptors. *Cell*. 2017 Jul 27;170(3):457–469.e13. <https://doi.org/10.1016/j.cell.2017.07.002>
13. Isaikina P, Petrovic I, Jakob RP, Sarma P, Ranjan A, Baruah M, et al. A key GPCR phosphorylation motif discovered in arrestin2-CCR5 phosphopeptide complexes. *Molecular Cell*. 2023 Jun 15;83(12):2108–2121.e7. <https://doi.org/10.1016/j.molcel.2023.05.002>
14. Min K, Yoon HJ, Park JY, Baidya M, Dwivedi-Agnihotri H, Maharana J, et al. Crystal Structure of  $\beta$ -Arrestin 2 in Complex with CXCR7 Phosphopeptide. *Structure*. 2020 Sep 1;28(9):1014–1023.e4. <https://doi.org/10.1016/j.str.2020.06.002>
15. Mayer D, Damberger FF, Samarasinghareddy M, Feldmueller M, Vuckovic Z, Flock T, et al. Distinct G protein-coupled receptor phosphorylation motifs modulate arrestin affinity and activation and global conformation. *Nat Commun*. 2019 Mar 19;10(1):1261. <https://doi.org/10.1038/s41467-019-09204-y>
16. Maharana J, Sarma P, Yadav MK, Saha S, Singh V, Saha S, et al. Structural snapshots uncover a key phosphorylation motif in GPCRs driving  $\beta$ -arrestin activation. *Molecular Cell*. 2023 Jun;83(12):2091–2107.e7. <https://doi.org/10.1016/j.molcel.2023.04.025>
17. Zheng C, Javitch JA, Lambert NA, Donthamsetti P, Gurevich VV. In-Cell Arrestin-Receptor Interaction Assays. *Current Protocols*. 2023;3(10):e890. <https://doi.org/10.1002/cpz1.8900.1002/cpz1.890>
18. Drube J, Haider RS, Matthees ESF, Reichel M, Zeiner J, Fritzwanker S, et al. GPCR kinase knockout cells reveal the impact of individual GRKs on arrestin binding and GPCR regulation. *Nat Commun*. 2022 Jan 27;13(1):540. <https://doi.org/10.1038/s41467-022-28152-8>



19. Lee Y, Warne T, Nehmé R, Pandey S, Dwivedi-Agnihotri H, Chaturvedi M, et al. Molecular basis of  $\beta$ -arrestin coupling to formoterol-bound  $\beta$ 1-adrenoceptor. *Nature*. 2020 Jul;583(7818):862–6. <https://doi.org/10.1038/s41586-020-2419-1>
20. Huang W, Masureel M, Qu Q, Janetzko J, Inoue A, Kato HE, et al. Structure of the neurotensin receptor 1 in complex with  $\beta$ -arrestin 1. *Nature*. 2020 Mar 12;579(7798):303–8. <https://doi.org/10.1038/s41586-020-1953-1>
21. Staus DP, Hu H, Robertson MJ, Kleinhenz ALW, Wingler LM, Capel WD, et al. Structure of the M2 muscarinic receptor– $\beta$ -arrestin complex in a lipid nanodisc. *Nature*. 2020 Mar 12;579(7798):297–302. <https://doi.org/10.1038/s41586-020-1954-0>
22. Bous J, Fouillen A, Orcel H, Trapani S, Cong X, Fontanel S, et al. Structure of the vasopressin hormone-V2 receptor– $\beta$ -arrestin1 ternary complex. *Sci Adv*. 2022 Sep 2;8(35):eabo7761. <https://doi.org/10.1126/sciadv.abo7761>
23. Liao YY, Zhang H, Shen Q, Cai C, Ding Y, Shen DD, et al. Snapshot of the cannabinoid receptor 1-arrestin complex unravels the biased signaling mechanism. *Cell*. 2023 Dec;186(26):5784–5797.e17. <https://doi.org/10.1016/j.cell.2023.11.017>
24. Maharana J, Sano FK, Sarma P, Yadav MK, Duan L, Stepniowski TM, et al. Molecular insights into atypical modes of  $\beta$ -arrestin interaction with seven transmembrane receptors. *Science*. 2024 Jan 5;383(6678):101–8. <https://doi.org/10.1126/science.adj3347>
25. Cao C, Barros-Álvarez X, Zhang S, Kim K, Dämgen MA, Panova O, et al. Signaling snapshots of a serotonin receptor activated by the prototypical psychedelic LSD. *Neuron*. 2022 Oct 5;110(19):3154–3167.e7. <https://doi.org/10.1016/j.neuron.2022.08.006>
26. Chen K, Zhang C, Lin S, Yan X, Cai H, Yi C, et al. Tail engagement of arrestin at the glucagon receptor. *Nature*. 2023 Aug;620(7975):904–10. <https://doi.org/10.1038/s41586-023-06420-x>
27. Kang Y, Zhou XE, Gao X, He Y, Liu W, Ishchenko A, et al. Crystal structure of rhodopsin bound to arrestin by femtosecond X-ray laser. *Nature*. 2015 Jul 30;523(7562):561–7. <https://doi.org/10.1038/nature14656>
28. Latorraca NR, Venkatakrishnan AJ, Dror RO. GPCR Dynamics: Structures in Motion. *Chem Rev*. 2017 Jan 11;117(1):139–55. <https://doi.org/10.1021/acs.chemrev.6b00177>
29. Latorraca NR, Wang JK, Bauer B, Townshend RJL, Hollingsworth SA, Olivieri JE, et al. Molecular mechanism of GPCR-mediated arrestin activation. *Nature*. 2018 May;557(7705):452–6. <https://doi.org/10.1038/s41586-018-0077-3>
30. Asher WB, Terry DS, Gregorio GGA, Kahsai AW, Borgia A, Xie B, et al. GPCR-mediated  $\beta$ -arrestin activation deconvoluted with single-molecule precision. *Cell*. 2022 May 12;185(10):1661–1675.e16. <https://doi.org/10.1016/j.cell.2022.03.042>
31. Shiraishi Y, Kofuku Y, Ueda T, Pandey S, Dwivedi-Agnihotri H, Shukla AK, et al. Biphasic activation of  $\beta$ -arrestin 1 upon interaction with a GPCR revealed by methyl-TROSY NMR. *Nat Commun*. 2021 Dec 9;12(1):7158. <https://doi.org/10.1038/s41467-021-27482-3>
32. Shukla AK, Manglik A, Kruse AC, Xiao K, Reis RI, Tseng WC, et al. Structure of active  $\beta$ -arrestin-1 bound to a G-protein-coupled receptor phosphopeptide. *Nature*. 2013 May;497(7447):137–41. <https://doi.org/10.1038/nature12120>
33. Zhai R, Wang Z, Chai Z, Niu X, Li C, Jin C, et al. Distinct activation mechanisms of  $\beta$ -arrestin-1 revealed by 19F NMR spectroscopy. *Nat Commun*. 2023 Nov 29;14(1):7865. <https://doi.org/10.1038/s41467-023-43694-1>
34. Asai D, Toita R, Murata M, Katayama Y, Nakashima H, Kang JH. Peptide substrates for G protein-coupled receptor kinase 2. *FEBS Letters*. 2014 Jun 13;588(13):2129–32. <https://doi.org/10.1016/j.febslet.2014.04.038>
35. Chen Q, Plasencia M, Li Z, Mukherjee S, Patra D, Chen CL, et al. Structures of rhodopsin in complex with G-protein-coupled receptor kinase 1. *Nature*. 2021 Jul;595(7868):600–5. <https://doi.org/10.1038/s41586-021-03721-x>
36. Duan J, Liu H, Zhao F, Yuan Q, Ji Y, Cai X, et al. GPCR activation and GRK2 assembly by a biased intracellular agonist. *Nature*. 2023 Aug;620(7974):676–81. <https://doi.org/10.1038/s41586-023-06395-9>
37. Baidya M, Kumari P, Dwivedi-Agnihotri H, Pandey S, Chaturvedi M, Stepniowski TM, et al. Key phosphorylation sites in GPCRs orchestrate the contribution of  $\beta$ -Arrestin 1 in ERK1/2 activation. *EMBO Rep*. 2020 Sep 3;21(9):e49886. <https://doi.org/10.15252/embr.201949886>

38. Møller TC, Pedersen MF, van Senten JR, Seiersen SD, Mathiesen JM, Bouvier M, et al. Dissecting the roles of GRK2 and GRK3 in  $\mu$ -opioid receptor internalization and  $\beta$ -arrestin2 recruitment using CRISPR/Cas9-edited HEK293 cells. *Sci Rep*. 2020 Oct 15;10(1):17395. <https://doi.org/10.1038/s41598-020-73674-0>
39. Doudna JA, Charpentier E. The new frontier of genome engineering with CRISPR-Cas9. *Science*. 2014 Nov 28;346(6213):1258096. <https://doi.org/10.1126/science.1258096>
40. Gusach A, García-Nafria J, Tate CG. New insights into GPCR coupling and dimerisation from cryo-EM structures. *Current Opinion in Structural Biology*. 2023 Jun;80:102574. <https://doi.org/10.1016/j.sbi.2023.102574>
41. Shukla AK, Westfield GH, Xiao K, Reis RI, Huang LY, Tripathi-Shukla P, et al. Visualization of arrestin recruitment by a G-protein-coupled receptor. *Nature*. 2014 Aug 14;512(7513):218–22. <https://doi.org/10.1038/nature13430>
42. Thomsen ARB, Plouffe B, Cahill TJ, Shukla AK, Tarrasch JT, Dosey AM, et al. GPCR-G Protein- $\beta$ -Arrestin Super-Complex Mediates Sustained G Protein Signaling. *Cell*. 2016 Aug;166(4):907–19. <https://doi.org/10.1016/j.cell.2016.07.004>
43. He QT, Xiao P, Huang SM, Jia YL, Zhu ZL, Lin JY, et al. Structural studies of phosphorylation-dependent interactions between the V2R receptor and arrestin-2. *Nat Commun*. 2021 Apr 22;12(1):2396. <https://doi.org/10.1038/s41467-021-22731-x>
44. García-Nafria J, Tate CG. Structure determination of GPCRs: cryo-EM compared with X-ray crystallography. *Biochemical Society Transactions*. 2021 Nov 1;49(5):2345–55. <https://doi.org/10.1042/BST20210431>
45. Janetzko J, Kise R, Barsi-Rhyne B, Siepe DH, Heydenreich FM, Kawakami K, et al. Membrane phosphoinositides regulate GPCR- $\beta$ -arrestin complex assembly and dynamics. *Cell [Internet]*. 2022 Nov 10 [cited 2022 Nov 11]; <https://doi.org/10.1016/j.cell.2022.10.018>
46. Nguyen AH, Thomsen ARB, Cahill TJ, Huang R, Huang LY, Marcink T, et al. Structure of an endosomal signaling GPCR-G protein- $\beta$ -arrestin megacomplex. *Nat Struct Mol Biol*. 2019 Dec;26(12):1123–31. <https://doi.org/10.1038/s41594-019-0330-y>
47. Cahill TJ, Thomsen ARB, Tarrasch JT, Plouffe B, Nguyen AH, Yang F, et al. Distinct conformations of GPCR- $\beta$ -arrestin complexes mediate desensitization, signaling, and endocytosis. *Proceedings of the National Academy of Sciences*. 2017 Mar 7;114(10):2562–7. <https://doi.org/10.1073/pnas.1701529114>
48. Ranjan R, Dwivedi H, Baidya M, Kumar M, Shukla AK. Novel Structural Insights into GPCR- $\beta$ -Arrestin Interaction and Signaling. *Trends in Cell Biology*. 2017 Nov 1;27(11):851–62. <https://doi.org/10.1016/j.tcb.2017.05.008>
49. Chen Q, Schafer CT, Mukherjee S, Gustavsson M, Agrawal P, Yao XQ, et al. ACKR3-arrestin2/3 complexes reveal molecular consequences of GRK-dependent barcoding [Internet]. *bioRxiv*; 2023 [cited 2024 May 7]. p. 2023.07.18.549504. <https://doi.org/10.1101/2023.07.18.549504>
50. Shihoya W, Iwama A, Sano FK, Nureki O. Cryo-EM advances in GPCR structure determination. *J Biochem [Internet]*. [cited 2024 Jun 14]; <https://doi.org/10.1093/jb/mvae029>
51. Grimes J, Koszegi Z, Lanoiselée Y, Miljus T, O'Brien SL, Stepniwski TM, et al. Plasma membrane preassociation drives  $\beta$ -arrestin coupling to receptors and activation. *Cell*. 2023 May 11;186(10):2238–2255.e20. <https://doi.org/10.1016/j.cell.2023.04.018>
52. Yin W, Li Z, Jin M, Yin YL, de Waal PW, Pal K, et al. A complex structure of arrestin-2 bound to a G protein-coupled receptor. *Cell Res*. 2019 Dec;29(12):971–83. <https://doi.org/10.1038/s41422-019-0256-2>
53. Wang Y, Wu L, Wang T, Liu J, Li F, Jiang L, et al. Cryo-EM structure of cannabinoid receptor CB1- $\beta$ -arrestin complex. *Protein & Cell*. 2024 Mar 1;15(3):230–4. <https://doi.org/10.1093/procel/pwad055>
54. Hurowitz EH, Melnyk JM, Chen YJ, Kouros-Mehr H, Simon MI, Shizuya H. Genomic Characterization of the Human Heterotrimeric G Protein  $\alpha$ ,  $\beta$ , and  $\gamma$  Subunit Genes. *DNA Research*. 2000 Jan 1;7(2):111–20. <https://doi.org/10.1093/dnares/7.2.111>

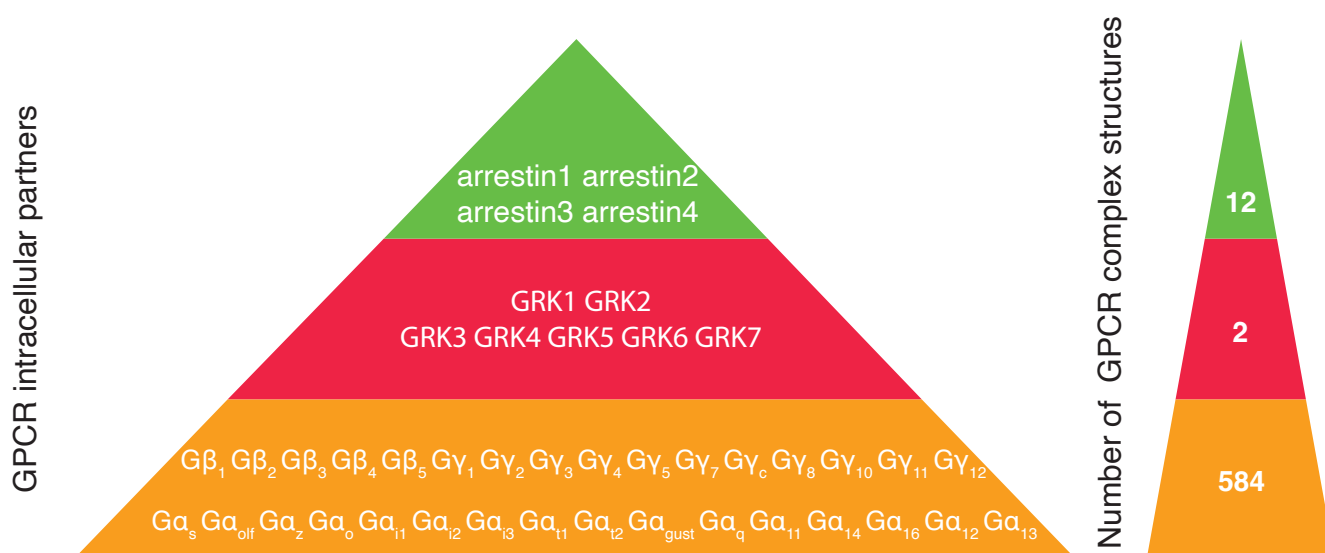
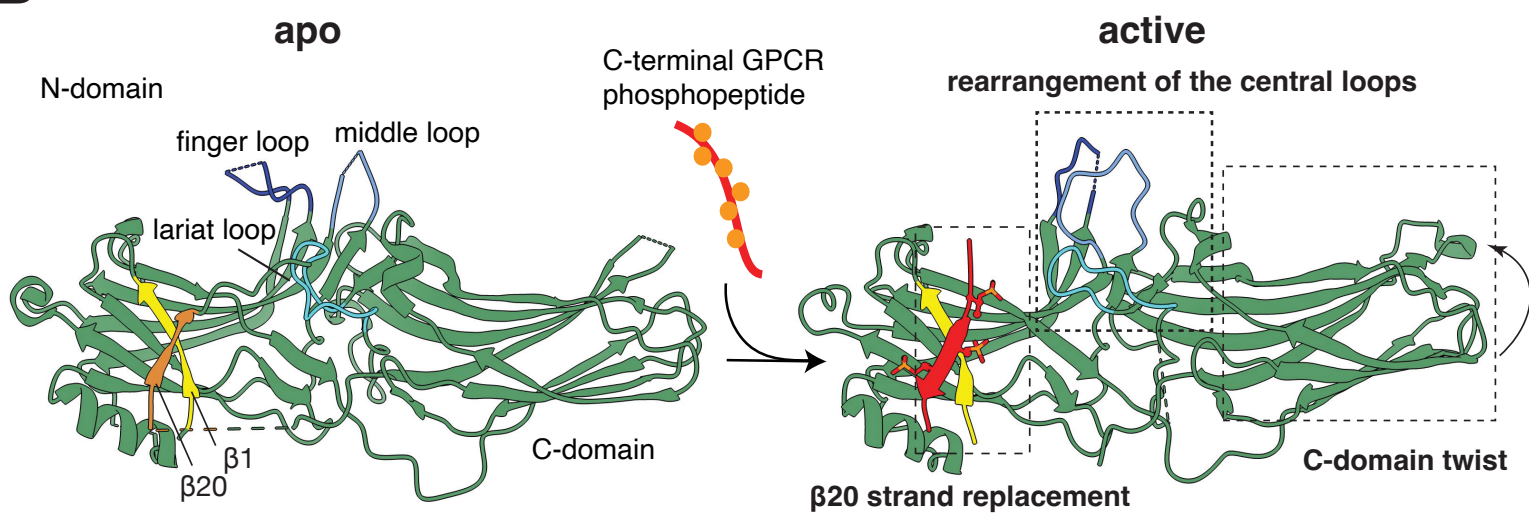
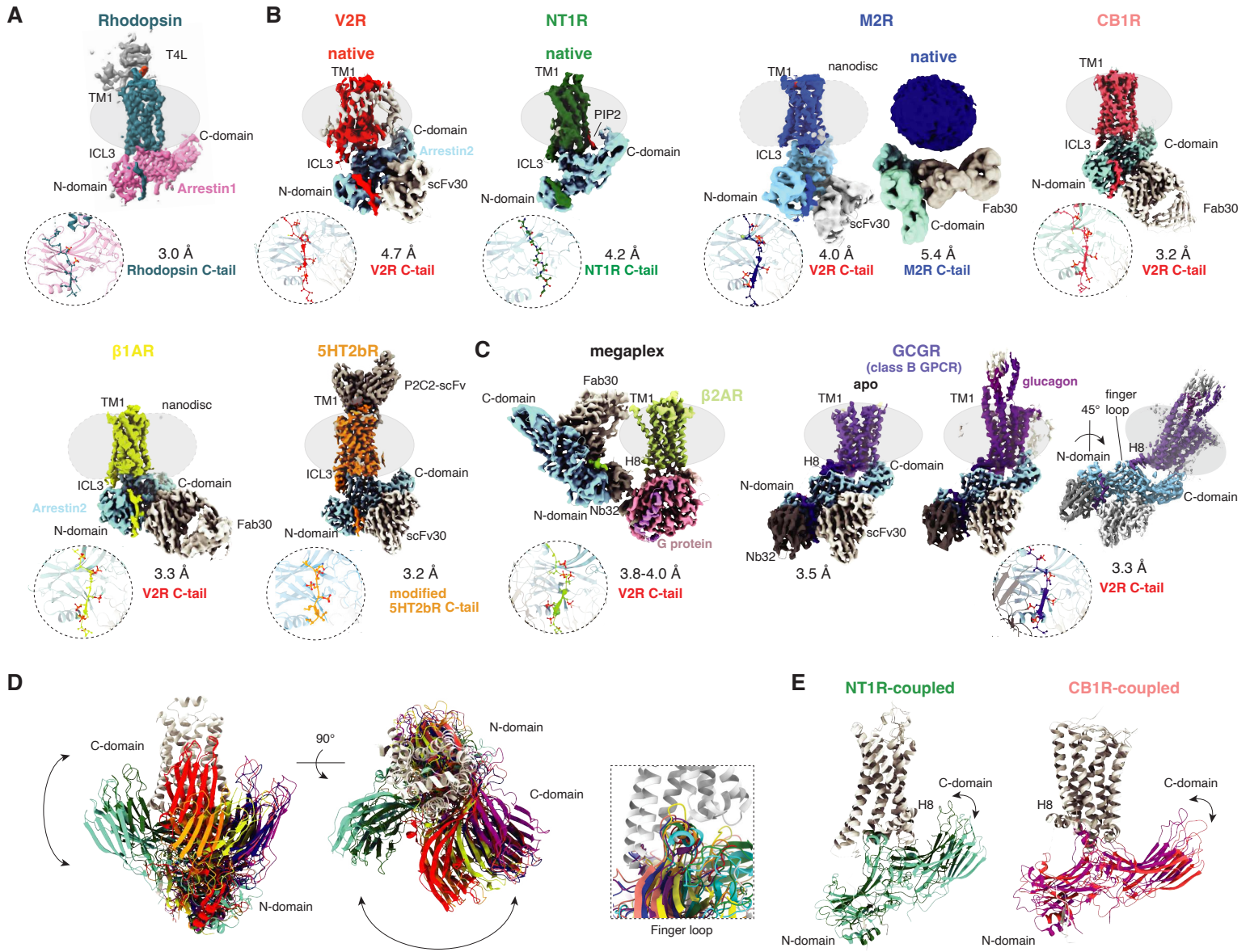
**A****B**

Figure 1



|                | GPCR      | ICL3 | C-term | GPCR      | ICL3 | C-term          |                 | GPCR              | ICL3 | C-term |
|----------------|-----------|------|--------|-----------|------|-----------------|-----------------|-------------------|------|--------|
| <b>Class A</b> | 5-HT1B    | x    | -      | CCR7      | -    | x               | <b>Class B1</b> | GPR153            | -    | x      |
|                | 5-HT1F    | x    | -      | CCR8      | -    | x               |                 | GPR161            | x    | x      |
|                | 5-HT2A    | x    | -      | CXCR1     | -    | x               |                 | GPR174            | -    | x      |
|                | 5-HT2B    | x    | -      | CXCR2     | -    | x               |                 | GPR182            | -    | x      |
|                | 5-HT4R    | -    | x      | CXCR3     | -    | x               |                 | GPR183            | -    | x      |
|                | M1R       | x    | -      | CXCR4     | -    | x               |                 | LGR4              | -    | x      |
|                | M2R       | x    | -      | CXCR5     | -    | x               |                 | LGR5              | -    | x      |
|                | M3R       | x    | -      | ACKR2     | -    | x               |                 | MRGPRX2           | -    | x      |
|                | M5R       | x    | -      | FSHR      | -    | x               |                 | P2RY10            | -    | x      |
|                | α1A-ADR   | -    | x      | LHR       | -    | x               |                 | TAAR8             | -    | x      |
|                | α1B-ADR   | x    | -      | PKR2      | -    | x               |                 | TAAR9             | -    | x      |
|                | α2A-ADR   | x    | -      | FFA4      | -    | x               |                 | calcitonin like-R | -    | x      |
|                | α2B-ADR   | x    | -      | BLT1R     | -    | x               |                 | GLP-1R            | -    | x      |
|                | α2C-ADR   | x    | -      | CysLT1R   | -    | x               |                 | secretin R        | -    | x      |
|                | β1-ADR    | -    | x      | LPA1R     | -    | x               |                 | PTH1R             | -    | x      |
|                | D2R       | x    | -      | LPA5R     | -    | x               | PTH2R           | -                 | x    |        |
|                | H1R       | x    | -      | S1P2R     | -    | x               | PAC1R           | -                 | x    |        |
|                | H3R       | x    | -      | S1P3R     | -    | x               | VPAC1R          | -                 | x    |        |
|                | H4R       | x    | x      | S1P4R     | -    | x               | VPAC2R          | -                 | x    |        |
|                | AT1R      | -    | x      | S1P5R     | x    | x               | ADGRL1          | -                 | x    |        |
|                | apelin R  | -    | x      | CB1R      | -    | x               | ADGRL2          | -                 | x    |        |
|                | BB2R      | -    | x      | GPR119    | -    | x               | ADGRL3          | -                 | x    |        |
|                | BB3R      | -    | x      | DP1R      | -    | x               | ADGRE1          | -                 | x    |        |
|                | CCK1R     | x    | -      | DP2R      | -    | x               | ADGRE2          | -                 | x    |        |
|                | CCK2R     | -    | x      | EP1R      | x    | -               | ADGRE3          | -                 | x    |        |
|                | C3AR      | -    | x      | EP2R      | -    | x               | ADGRE5          | -                 | x    |        |
|                | C5A1R     | -    | x      | EP3R      | -    | x               | ADGRA2          | -                 | x    |        |
|                | FPR1      | -    | x      | EP4R      | -    | x               | ADGRA3          | -                 | x    |        |
|                | FPR3      | -    | x      | FPR       | -    | x               | CELSR1          | -                 | x    |        |
|                | ghrelin R | -    | x      | A1R       | x    | -               | CELSR2          | -                 | x    |        |
|                | motilin R | -    | x      | P2Y2R     | -    | x               | CELSR3          | -                 | x    |        |
|                | NMU1R     | -    | x      | P2Y4R     | -    | x               | ADGRD1          | -                 | x    |        |
|                | NPFF2R    | -    | x      | P2Y12R    | -    | x               | ADGRF5          | -                 | x    |        |
|                | Y1R       | -    | x      | P2Y13R    | -    | x               | ADGRB1          | -                 | x    |        |
|                | Y5R       | x    | -      | GPBAR     | -    | x               | ADGRB2          | -                 | x    |        |
|                | NTS1R     | -    | x      | Rhodopsin | -    | x               | ADGRB3          | x                 | x    |        |
|                | OX1R      | -    | x      | OPN4      | -    | x               | ADGRG1          | -                 | x    |        |
|                | OX2R      | -    | x      | OPN5      | -    | x               | ADGRG2          | -                 | x    |        |
|                | PAR1      | -    | x      | OPN1SW    | -    | x               | ADGRG3          | -                 | x    |        |
|                | PAR2      | -    | x      | OPN1MW    | -    | x               | ADGRG4          | -                 | x    |        |
|                | PAR4      | -    | x      | OPN1LW    | -    | x               | ADGRG5          | -                 | x    |        |
|                | RXFP1     | -    | x      | GPR4      | x    | -               | ADGRG6          | -                 | x    |        |
|                | RXFP2     | -    | x      | GPR15     | -    | x               | ADGRG7          | -                 | x    |        |
|                | RXFP3     | -    | x      | GPR19     | -    | x               | ADGRV1          | -                 | x    |        |
|                | SST1R     | -    | x      | GPR22     | x    | -               | CASR            | -                 | x    |        |
| SST4R          | -         | x    | GPR25  | -         | x    | GABA-B1         | x               | x                 |      |        |
| NK1R           | -         | x    | GPR34  | -         | x    | GABA-B2         | -               | x                 |      |        |
| NK2R           | -         | x    | GPR37  | -         | x    | mGlu1R          | -               | x                 |      |        |
| NK3R           | -         | x    | GPR50  | -         | x    | mGlu2R          | -               | x                 |      |        |
| UTR            | -         | x    | GPR61  | x         | -    | mGlu3R          | -               | x                 |      |        |
| V1AR           | -         | x    | GPR65  | -         | x    | mGlu5R          | -               | x                 |      |        |
| V1BR           | x         | x    | GPR75  | -         | x    | mGlu7R          | -               | x                 |      |        |
| V2R            | -         | x    | GPR82  | x         | -    | mGlu8R          | -               | x                 |      |        |
| OTR            | -         | x    | GPR101 | x         | -    | GPR156          | -               | x                 |      |        |
| CCR1           | -         | x    | GPR139 | -         | x    | GPR158          | -               | x                 |      |        |
| CCR3           | -         | x    | GPR149 | x         | x    | GPR179          | -               | x                 |      |        |
| CCR4           | -         | x    | GPR151 | -         | x    | GPRC6           | -               | x                 |      |        |
| CCR5           | -         | x    | GPR152 | -         | x    | FZD8            | -               | x                 |      |        |
|                |           |      |        |           |      | <b>Class B2</b> |                 |                   |      |        |
|                |           |      |        |           |      | <b>Class C</b>  |                 |                   |      |        |
|                |           |      |        |           |      | <b>Class F</b>  |                 |                   |      |        |

Figure 3